The Isomerization Barrier in Cyanocyclobutadienes: An ab Initio Multireference Average Quadratic Coupled Cluster Study

Mirjana Eckert-Maksić,*,† Hans Lischka,*,‡,§ Zvonimir B. Maksić,|| and Mario Vazdar†

Laboratory for Physical Organic Chemistry, Division of Organic Chemistry and Biochemistry, Rudjer Bošković Institute, POB 108, HR-10002 Zagreb, Croatia, Institute of Organic Chemistry and Biochemistry, Academy of Sciences of the Czech Republic, Flemingovo nam. 2, CZ-16610 Prague 6, Czech Republic, Institute for Theoretical Chemistry, University of Vienna, Währingerstrasse 17, A-1090 Vienna, Austria, and Quantum Organic Chemistry Group, Division of Organic Chemistry and Biochemistry, Rudjer Bošković Institute, POB 108, HR-10002 Zagreb, Croatia

Received: February 19, 2009; Revised Manuscript Received: May 25, 2009

The energy profiles of the isomerization of mono, di-, and tetracyano-substituted cyclobutadienes (CBDs) are computed at the multireference average quadratic coupled cluster/complete active space self-consistent field level of theory. It was found that the energy barrier heights for the automerization reaction are 2.6 (tetracyano-CBD), 5.1 (1,3-dicyano-CBD), and 6.4 (cyano-CBD) kcal mol^{-1}, implying that they are lowered relative to that in the parent CBD (6.4 kcal mol^{-1}), the monosubstituted derivative being an exception. Since the free CBD shuttles between two equivalent structures even at low temperature of 10 K, it follows that bond-stretch isomerism does not take place in cyanocyclobutadienes. Instead, these compounds exhibit rapid fluxional interconversion at room temperature between two bond-stretch isomers by the double bond flipping mechanism. The reason behind the decrease in the barrier heights is identified as a slightly enhanced resonance effect at the saddle points separating two (equivalent) bond-stretch isomers, compared to that in the equilibrium structures, predominantly due to the diradical character of the former. It is also shown that the energy gap between the singlet ground state saddle point structure and the first triplet equilibrium geometry decreases upon multiple substitution by the cyano groups. The splitting of the S and T energy is small being within the range of 6.5−8.2 kcal mol^{-1}.

Introduction

Cyclobutadiene (CBD) **1** is the second smallest highly strained organic ring compound,[1] which serves also as a prototype of antiaromatic systems due to its 4π electrons.[2,3] The combination of these two facets leads to a number of unusual properties, which have intrigued researchers for decades.[4] A very recent attempt of measuring the heat of formation of CBD[5] and some comments on the nature of its antiaromaticity[6] witness continuing interest on the topic illustrating the fact that some controversies are still going on. Substituted CBDs represent also good candidates for systems exhibiting bond-stretch isomerism, i.e., that two stable structures differ only in their bond distances. This is a point of considerable importance, in particular since there is an ongoing debate whether bond-stretch isomers are facts or artifacts.[7−10] The experimental evidence is sparse, but it is now unequivocally established that two 1,2- and 1,8-dichloroperfluorocyclooctatetraene[11] are true bond-stretched isomers. The same holds for 1,3-diphosphabicyclobutane-2,4-diyl- and 1,3-diphosphabicyclo[1.1.0]-butanes.[12−15] Detailed calculations performed in our group based on the multireference average quadratic coupled cluster (MR-AQCC) method have been performed on benzo[1,2:4,5]dicyclobutadiene.[16] It was found that the two bond-stretch isomers are minima on the energy hypersurface, but they were separated by a barrier height of only 5 kcal mol^{-1} implying that their existence in solution at room temperature is questionable. They most likely form a fluxional system with a permanent interconversion. Borden and Davidson[17] considered *t*-butyl substituted CBD and found that the barrier was lowered relative to parent cyclobutadiene. Clearly, this derivative is also a fluxional system just like the parent CBD[18] since it was shown by Arnold and Michl that the latter undergoes rapid bond flipping interconversions at 10 K. It was argued that the reason behind a decreased barrier of *t*-butyl derivative was increased steric repulsion between the bulky substituents in the energy minimum relative to that in the saddle point.[17] In other words, the transition state is less destabilized by substituents than the equilibrium structure. It is of interest to examine influence of other substituents on the barrier heights. Before doing that, it is necessary to obtain an estimate of the barrier of automerization of CBD as accurately as possible.

Despite its seemingly simple electronic and spatial structure of high symmetry, the theoretical description of CBD requires advanced post-Hartree−Fock methods. Furthermore, if the barrier of the automerization reaction is considered, multiconfiguration and multireference computational schemes should be applied to the ground state minimum (GS), the corresponding saddle point (SP), and the first triplet state (1TS) at their optimized structures for balanced calculations of the energy profile of the same accuracy. The reason behind is that the saddle point on the potential energy surface (PES), which is of quadratic structure (D_{4h}), possesses a significant diradical character, being

* To whom correspondence should be addressed. E-mail: mmaksic@emma.irb.hr (M.E.-M.); hans.lischka@univie.ac.at (H.L.).

† Laboratory for Physical Organic Chemistry, Division of Organic Chemistry and Biochemistry, Rudjer Bošković Institute.

‡ Academy of Sciences of the Czech Republic.

§ University of Vienna.

|| Quantum Organic Chemistry Group, Division of Organic Chemistry and Biochemistry, Rudjer Bošković Institute.

10.1021/jp9015273 CCC: $40.75
Published on Web 07/01/2009

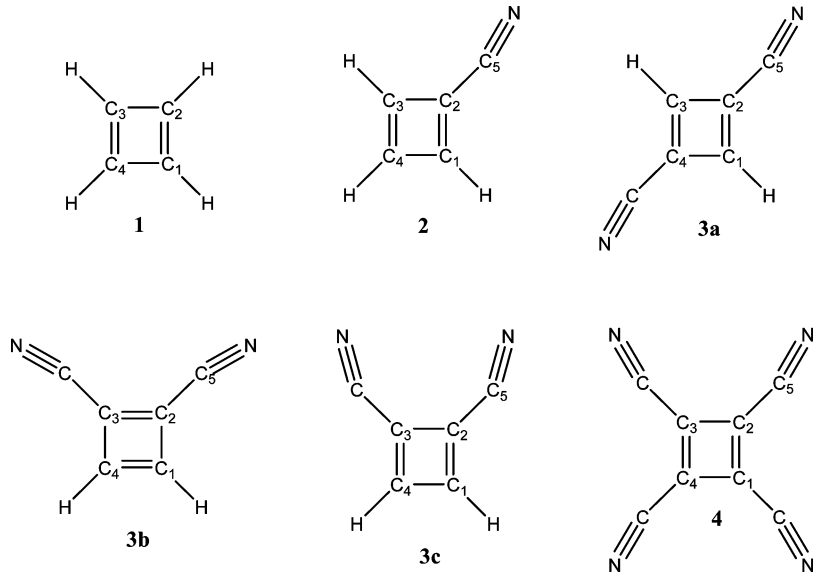

Figure 1. Schematic representation and numbering of atoms in cyclobutadiene and its mono-, di-, and tetrasubstituted cyano derivatives.

close in energy to the first triplet excited state. This problem aroused interest of both experimentalists and theoreticians. The experimentally determined barrier height in cyclobutadiene lies in the range between 1.6−10 kcal mol^{-1} depending on the substituents.[19,20] Theoretical results also vary owing to widely different methods, which have been employed. The most recent benchmark value[21] obtained by the MR-AQCC method and basis set extrapolation including zero-point vibration energy (ZPVE) correction was 6.3 kcal mol^{-1}.[21] The multireference Brillouin−Wigner coupled cluster MR-BWCCSD(T)/cc-pVTZ method involving noniterative triples gave a barrier height of 4.5 kcal mol^{-1} as obtained by Demel and Pittner,[22] if the ZPVE correction (2.5 kcal mol^{-1}) computed in ref 21 is taken into account. This is 0.5 kcal mol^{-1} higher than the earlier result of Balková and Bartlett,[23] provided the same ZPVE correction is used,[21] but it differs by 1.8 kcal mol^{-1} from the MR-AQCC benchmark result of 6.3 kcal mol^{-1}. It should be noted that the latter value lies practically in the middle of the experimental range. Obviously, some substituents decrease the barrier, whereas others increase it. Finally, it has been shown by the ^{13}C NMR experiment at 88 K[24] that the barrier for tri-*t*-butylcyclobutadiene was not larger than 2.5 kcal mol^{-1} in accordance with theoretical prediction.[17] It should be noted in passing that the electronic energy barrier height for permethyl-CBD was computed by the MC-SCF(4,4)/6-31++G(d,p) method recently[25] and a value of 6.8 kcal mol^{-1} was obtained. It is reduced to 3.7 kcal mol^{-1}, if the ZPVE contribution is included, thus implying that the system is fluxional too.

It is the aim of this work to concentrate on spatially compact groups like CN, which are not sterically demanding and lead to planar structures enabling π conjugation. Consequently, they should affect the barriers differently than alkyl substituents. Anticipating forthcoming results, this surmise was correct. The effect of cyano groups was studied for the series of mono-, di-, and tetrasubstituted cyclobutadienes in order to contribute toward better understanding of the influence of highly electronegative substituents on this interesting phenomenon called bond-stretch isomerism.

Computational Methods

Complete active space self-consistent field (CASSCF)[26−28] and multireference averaged coupled cluster MR-AQCC[29−31] calculations were carried out on the parent CBD (**1**) for comparative purpose and its derivatives **2**−**4** (Figure 1). A distinct advantage of the adopted method is a combination of multiconfiguration and multireference calculations involving approximate size extensivity effect correction, thus leading to a balanced description of the nondynamic and dynamic electron correlation contributions provided sufficiently flexible basis sets are used. Additionally, the availability of the analytic energy gradients[29−31] allows geometry optimization and location of the saddle point structures at a very high level of theory enabling in this way an accurate energy follow-up along the reaction pathway. Different complete active spaces for different molecules were used in the CASSCF calculations depending on the number of π electrons, basis set functions and spatial symmetry of the studied system. The CASSCF(4,4) and CASSCF(12,12) calculations were performed for **1** and **4**, respectively, where the first number within parentheses denotes the number of π electrons, while the second gives the number of active π orbitals. For system **2**, CASSCF(6,6) calculations have been performed, whereas in disubstituted derivatives **3a, 3b**, and **3c,** CASSCF(8,8) wave functions have been used. It should be mentioned that the molecular orbitals describing the CAS were of π and π^* type, since it has been demonstrated that this orbital manifold was sufficient in the case of free CBD.[21] The final expansion space in the MR-AQCC computations in terms of the configuration state functions (CSFs) comprised the configurations obtained from a CAS(4,4) reference space and the configurations obtained by all single and double electron excitations into internal and external orbitals (MR-AQCC(4,4)). Orbitals used in the reference space were selected according to the CASSCF natural occupations. In systems with more than four π centers, those orbitals with natural occupation number close to two (within a threshold of 0.05) were considered as doubly occupied orbitals, whereas the orbitals with natural occupation number close to zero (again within a threshold of 0.05), were moved into the virtual space. In that way, the reference space with four π-electrons in four π-orbitals is formed and used throughout all MR-AQCC calculations. The core $(1s)^2_C$ and $(1s)^2_N$ electrons were kept frozen. The symmetry of the reference configurations was confined to the state symmetry. It should be mentioned that three-substituted CBD was not considered in view of its low

TABLE 1: Relevant Structural Parameters of CBD and Its Cyano Derivatives as Obtained by the MR-AQCC(4,4)/SS-CASSCF/6-31G(d) Method (Distances in Ångstroms, Angles in Degrees)[a]

	1	2	Δ(2)	3a	Δ(3a)	3b	Δ(3b)	3c	Δ(3c)	4	Δ(4)
d(C1−C2)	1.356	1.363	0.007	1.362	0.006	1.553	−0.009	1.366	0.010	1.371	0.015
d(C2−C3)	1.562	1.567	0.005	1.555	−0.007	1.372	0.016	1.563	0.001	1.546	−0.016
d(C3−C4)	1.356	1.355	−0.001	1.362	0.006	1.553	−0.009	1.366	0.010	1.371	0.015
d(C1−C4)	1.562	1.550	−0.012	1.555	−0.007	1.355	−0.001	1.544	−0.018	1.546	−0.016
d(C2−C5)		1.418		1.419		1.417		1.421		1.414	
d(C5−N)		1.174		1.171		1.171		1.172		1.171	
C1−C2−C3	90.0	89.7	−0.3	90.6	0.6	89.7	−0.3	89.6	−0.4	90.0	0
C2−C3−C4	90.0	89.5	−0.5	89.4	−0.6	90.3	0.3	90.4	0.4	90.0	0
C1−C2−C5		135.2		135.1		135.3		140.6		135.8	
C2−C5−N		178.6		178.6		181.6		173.4		178.8	

[a] The C_2−C_5≡N fragments are avoiding each other or are bent toward in **3b** and **3c** compounds, respectively, as evidenced by the corresponding bending angles of 181.6 and 173.4° (see text).

symmetry (C_s), which made calculations too demanding, if the larger basis set 6-311G(2d,p) is used. The interacting space restriction was employed as recommended by Bunge.[32]

Geometry optimizations were performed by using natural internal coordinates[33] and the GDIIS procedure.[34] Finally, it should be mentioned that the MR-AQCC calculations were based on Pople's 6-31G(d) and 6-311G(2d,p) functions,[35] which are expected to represent a fair compromise between efficiency and accuracy. The 6-31G(d) basis set has been used for geometry optimization and additional single point calculations were performed with the triple-ζ basis set.

The ZPVE corrections were computed at the CASSCF level. The active spaces were the same as in previous CASSCF calculations with one notable exception: in tetracyano derivative **4** the CASSCF(4,4) method was employed for economy reasons. Harmonic force constants were computed by finite differences of the energy gradients. The harmonic vibrational frequencies were obtained by the SUSCAL program developed by Pulay et al.[36] The minima on the potential energy surfaces were verified by the frequency analysis. The COLUMBUS suite of codes was used in energy calculations,[37−40] with the DALTON[41] program package providing the atomic one- and two electron integrals for energy and gradient calculations. The natural orbital (NBO) hybridization parameters were calculated using GAUSSIAN 03 suite of programs.[42]

Results and Discussion

The studied compounds are depicted in Figure 1. We shall commence discussion with the structural parameters of the energy minima in the ground states and the lowest triplet states, which will be subsequently followed by inspection of the saddle points and energetic scrutiny of the barrier heights. Finally, the singlet−triplet energy gaps will be considered.

Structures. The relevant geometric parameters of the parent CBD and its cyano derivatives in the ground state calculated by the MR-AQCC(4,4)/SS-CASSCF/6-31G(d) method are summarized in Table 1. The first important information is that all systems at equilibrium and saddle point structures are planar on the lowest singlet (ground-state) surface. The shape and symmetry of the geometric structures is of interest. Compounds **1** and **4** are rectangular (D_{2h}), whereas **3b** and **3c** are trapezoidal (C_{2v}). Isomer **3a** has the form of the parallelogram possessing C_{2h} symmetry. However, the deviations from the rectangular ring angles are tiny, being practically negligible in all cases (Table 1). The C−C≡N fragments exhibit interesting nonlinearities (Figure 1). The C−C≡N angles are important because they offer a useful probe of the intramolecular interactions. In particular, orientation of the C≡N grouping indicates repulsion in **2**, **3a**, and **3c** between the hydrogen and nitrogen atoms, which is larger over the C═C double bond than over C−C single bond. The repulsion between the nitrogens becomes decisive in **3b** and **4** being always stronger across the C═C short bond(s) as intuitively expected. Interestingly, the repulsion between N atoms in **3b** prevails over the repulsion between N and H atoms, whereas the opposite is the case in **3c**. The position of the C═C double bond is a useful diagnostic tool in this respect. The angles of deviation from 180° in C−C≡N fragments are small in **2** and **3a** being 1.4°. The C_2−C_5≡N angles in **3b** and **3c** are 181.6 and 173.4°, respectively, whereas in **4** they assume 178.8° (Figure 1).

The changes of the single and double bonds of the ring upon substitution are denoted by Δ (Table 1). They provide insight into the conjugation interaction between the cyano groups and the ring CC bonds combined with the rehybridization effect triggered by substitution. According to a general picture offerred by Pauling's zwitterionic resonance structures with nitrogens as anionic centers (Figure S1 of Supporting Information), the single bonds should be somewhat shortened, whereas the double bonds should be lengthened in the same vein. Let us consider system **3c** first, since it provides an instructive example. The C═C double bonds are stretched by 0.01 Å, whereas the C1−C4 single bond is shrunk by 0.02 Å. A factor of 2 is easily understood, because it is easier to shorten a weaker C−C single bond than to stretch a considerably stronger C═C double bond. Perusal of the bond distances in **3b** is interesting, because it illustrates a well known fact that the resonance effect is efficiently spread over the alternating double and single bonds, which in this particular case has a semicircular U shape (Figure S1 of Supporting Information). The C2═C3 bond is more lengthened (0.016 Å) than the C═C double bonds in **3c** (0.010 Å). In contrast, the C1═C4 double bond in **3b** is practically left unaltered. This is intuitively clear, because the C2═C3 double bond is under immediate influence of two directly attached CN groups. The influence of the resonance effect on the remote C1═C4 double bond is negligible. The structural changes found in disubstituted CBDs are balanced in tetracyanocyclobutadiene **4** (Table 1), meaning that the double and single CC bonds are legthened and shortened by the same amount (0.016 Å), respectively.

A useful bonding parameter is the s-character of the local hybrid orbitals. They are calculated by the natural bond orbital analysis (NBO)[43,44] by using B3LYP/6-311G(d) wave functions computed at the MR-AQCC(4,4)/SS-CASSCF/6-31G(d) geometric structure. The use of B3LYP methodology is justified, because the hybridization indices are highly insensitive to the quality of the wave function.[45] To illustrate this important point,

TABLE 2: Relevant Structural Data of the SP and the LTS Minima Calculated by the MR-AQCC(4,4)/SS-CASSCF/6-31G(d) (Distances in Ångstroms, Angles in Degrees)

	1SP	1LTS	2SP	2LTS	3aSP	$3LTS_a$	3SP	$3LTS_b$	$3LTS_c$	4SP
d(C1−C2)	1.451	1.445	1.449	1.459	1.451	1.446	1.454	1.449	1.452	1.453
d(C2−C3)	1.451	1.445	1.449	1.459	1.451	1.446	1.465	1.469	1.466	1.453
d(C3−C4)	1.451	1.445	1.428	1.443	1.451	1.446	1.454	1.449	1.452	1.453
d(C1−C4)	1.451	1.445	1.428	1.443	1.451	1.446	1.433	1.422	1.426	1.453
d(C2−C5)			1.409	1.412	1.414	1.414	1.410	1.407	1.411	1.409
d(C5−N)			1.174	1.174	1.172	1.172	1.173	1.174	1.176	1.172
C1−C2−C3	90.0	90.0	89.6	89.9	91.0	91.1	90.6	90.9	90.8	90.0
C2−C3−C4	90.0	90.0	89.5	89.5	89.0	88.9	89.4	89.1	89.2	90.0
C1−C2−C5			135.0	135.1	134.5	134.5	135.8	135.7	140.2	135.0

we have calculated s characters in some simple hydrocarbons including CBD by the HF, B3LYP, and MP2 methods employing 6-31G(d) basis set. These single-point calculations were carried out on the MP2/6-31G(d) geometries (Table S1 of Supporting Information). It turns out that the B3LYP and MP2 s characters differ from the Hartree−Fock ones by very small amounts. Obviously, the composition of the local hybrid orbitals does not depend on the electron correlation. The calculated s characters of the directed local hybrid orbitals will be used only in qualitative discussion. The results are given in Table S2 of Supporting Information. To rationalize these numbers it is necessary to invoke the Bent rule,[46] which says that the electronegative atom (nitrogen) prefers the hybrid atomic orbital with higher p character residing on the electropositive atom (carbon) placed forming the C−N covalent bond. This is the reason behind a finding that two hybrids located at the C5 atom possess different s characters. The hybrid with s content lower than 50% (∼47%) is directed toward nitrogen whereas the other one pointing toward the C2 atom has the s character larger than 50% (∼52%). As a consequence the hybrid residing on C2 being aligned along the C2−C5 bond has also the s content higher than 33.3%. This is a consequence of another rule, which states that two overlapping hybrids placed at atoms of comparable electronegativity lead to optimal bonding, if their s characters are as close as possible.[47] Concomitantly, the hybrids describing the ring bonds take lower s character compared to that in free CBD. The latter are 38.2% for the C=C double and 27.2% for the C−C single bonds, which provide a suitable gauge. It is useful to recall that higher s character implies shorter and stronger bonds, respectively.[48,49] Conversely, the increased p character contributes toward some lengthening of the C1=C2 and C3=C4 bonds, but it opposes the shortening of the C2−C3 and C1−C4 bonds. A scrutiny of the rehybridization effect reveals that it is fairly small and that the variation in bond distances discussed above is predominantly due to the π-electron resonance influence.

The relevant spatial structural parameters of the saddle points and the lowest triplet state minima are presented in Table 2. The saddle points are characterized by the single imaginary frequencies, which are given in Table S3 of Supporting Information. Perusal of the data reveals that geometries of the saddle points (SP) on the singlet GS potential energy surface and the minima of the first triplet state are similar. Although compounds **3b** and **3c** have the same saddle point structure (3SP), their lowest triplet geometries $3LTS_b$ and $3LTS_c$ differ slightly.

The bond distances related to the cyano group *d*(C2−C5) and *d*(C5≡N) are of importance for diagnostic purpose. The triple cyano bond is changed by a very small amount because of its stiffness. Hence, a better monitor is given by the single C2−C5 bond which is more sensitive probe of the resonance effect. It is remarkable that the C2−C5 distance is decreased

TABLE 3: Total Electronic Energies (au.) of Molecules 1−4 as Obtained by CASSCF/6-31G(d)[a] and MR-AQCC(4,4)/6-311G(2d,p)//MR-AQCC(4,4)/6-31G(d)/CASSCF/6-31G(d) Calculations[b] with ZPVEs (in kcal mol^{-1}) Computed by the CASSCF/6-31G(d) Method[c]

	ground state		transition state		ZPVE	
	CASSCF	MR-AQCC	CASSCF	MR-AQCC	GS	TS
1	−153.70791	−154.29439	−153.69806	−154.28019	39.5	37.0
2	−245.47457	−246.34490	−245.46592	−246.33097	39.1	36.8
3a	−337.23506	−338.38027	−337.22738	−338.36810	38.5	36.0
3b	−337.23345	−338.37835	−337.22644	−338.36818	38.5	36.4
3c	−337.23310	−338.37734	−337.22644	−338.36818	38.5	36.4
4	−520.73871	−522.26393	−520.73344	−522.25647	38.4	36.3

[a] CASSCF calculations were performed with CAS(4,4) for molecule **1**, CAS(6,6) for molecule **2**, CAS(8,8) for molecules **3a**, **3b**, and **3c**, and CAS(12,12) for molecule **4**. Hereafter, it is abbreviated as CASSCF. [b] Tetracyanocyclobutadiene is considered at the MR-AQCC-(4,4)/6-31G(2d,p)//MR-AQCC(4,4)/6-31G(d)/CASSCF/6-31G(d) level of theory, since the single-point calculations with 6-311G(2d,p) basis set are not feasible. [c] ZPVEs are calculated with CASSCF calculation by using CAS(4,4) for molecules **1** and **4,** CAS(6,6) for molecule **2**, and CAS (8,8) for molecules **3a, 3b**, and **3c**.

in the saddle point **2SP**, **3aSP**, **3SP**, and **4SP** relative to the initial systems **2**, **3a**, **3b** (and **3c**), and **4**, respectively. This finding indicates an increase in the resonance effect at the saddle points, which will be discussed in the second to the next section (vide infra). The CC bond distance of the ring is by only 0.002 Å larger in the **4SP** saddle point than in the **1SP** of the parent CBD, which is negligible. Interestingly, the C2−C5≡N fragments are linear in all saddle points and the first triplet structures, which is intuitively expected, since the CC bond distances of the ring are equal being between the lengths of double and single bonds in the equilibrium geometries. Thus, the repulsions between either C−C≡N fragments themselves, or with the C−H bonds are balanced.

Energetic Properties. Let us consider the total electronic energies of compounds **1**−**4** for the equilibrium and saddle point geometries. They are given together with the corresponding ZPVEs in Table 3. The total energies are calculated at the single point MR-AQCC(4,4)/6-311G(2d,p)//MR-AQCC(4,4)/SS-CASSCF/6-31G(d) level, where SS stands for the single state. The ZPVEs are obtained by the CASSCF method described in the section Computational Methods. They are larger at the energy minima than at the saddle points as expected because one vibrational mode of imaginary frequency does not affect the latter. The difference ZPVE(minimum) − ZPVE(saddle point) is fairly constant assuming either a value of 2.5 kcal mol^{-1} for **1** and **3a**, 2.3 kcal mol^{-1} for **2,** or 2.1 kcal mol^{-1} in **3b**, **3c**, and **4** thus spanning a close range of 2.1−2.5 (in kcal mol^{-1}). The ZPVEs themselves are surprisingly constant, which is counterintuitive in view of additivity of this magnitude in terms of the atomic contributions[50−52] based on the model of spherical atoms. A

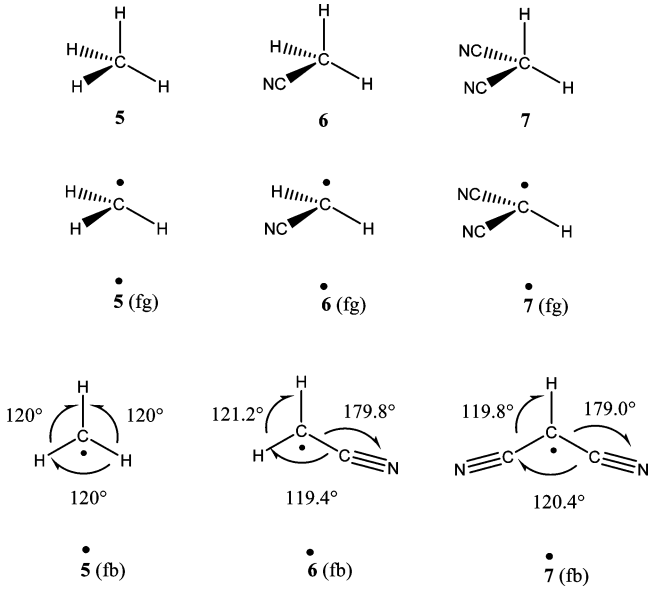

Figure 2. Schematic representation of CH_4 (**5**), CH_3CN (**6**), and $CH_2(CN)_2$ (**7**) and their frozen radicals obtained by the H atom abstraction **5**$^{\bullet}$ (fg), **6**$^{\bullet}$ (fg), and **7**$^{\bullet}$ (fg). The planar structures **5**$^{\bullet}$ (fb), **6**$^{\bullet}$ (fb), and **7**$^{\bullet}$ (fb) are result of the relaxation of bond angles.

refined treatment includes atoms in their different hybridization states,[53] which is more consistent with the concept of effective atomic force constants.[54,55] The refined formula works very well in small molecules. Accordingly, the ZPV energy should increase with the number of atoms. However, the multiple CN substitution slightly but persistently decreases the ZPVE values (Table 3). The reason for this unusual behavior is the following. In substituted cyano derivatives, the number of normal modes of vibration is larger. However, the analysis of the vibrational wave numbers shows that they are significantly lower than those in CBD for the CH streching modes. It turns out that a contribution of the large number of normal modes in cyano derivatives with smaller vibrational energies leads to fairly constant ZPVEs.

There are three dicyano derivatives **3a**, **3b**, and **3c**, which are given in decreasing hierarchy of stability. The differences in the total electronic energy between **3a** and **3b** against the least stable isomer **3c** at the MR-AQCC level are −1.9 and −0.8 kcal mol^{-1}, respectively, whereas **3a** is more stable than **3b** by 1.1 kcal mol^{-1}. We shall refrain from interpreting such subtle energy differences.

In conclusion, it should be reiterated that cyanation induces a stabilizing resonance effect, which is the largest in tetracyanocyclobutadiene. The effect can be qualitatively rationalized by a number of zwitterionic resonance structures, which leave their fingerprints in changes of the bond distances.

Automerization and Bond−Stretch Barriers. The barrier heights of the automerization reactions are of particular interest, because they are crucial for the existence of the isomers differing only in the bond length(s). The calculated structures of the saddle points indicate that the cyano groups trigger a resonance effect, which is stronger than in the equilibrium geometries. In particular, the shrinkage of the C2−C5 bond is larger revealing increased interaction between the cyano groups and diradical transition states, thus leading to lowering of the barriers. In order to illustrate stabilization of the cyano group(s) by the neighboring radical center, we shall consider radicals obtained by the homolitic bond rupture of the CH bond in methane **5** and its derivatives CH_3CN **6** and $CH_2(CN)_2$ **7** (Figure 2). Bond cleavage will be broken down to three steps. First, the H atom leaves, while the radicals are kept frozen at the structural parameters in the parent molecules. They are denoted by $\dot{C}H_n(CN)_{3-n}$ (n = 1,2,3). Subsequently, the relaxation of the radical is decomposed in two components: (a) the bond angles are optimized by keeping the bond distances still fixed, which yields the relaxation stabilization E_{rex}(angle), and (b) the clamped distance requirement is removed providing additional lowering of the radical energy denoted by E_{rex}(bond), which finally leads to the equilibrium structure. The total reorganization energy is a sum $E_{rex}(tot) = E_{rex}(angle) + E_{rex}(bond)$. The energies were calculated by the ROMP2/6-311+G(d,p)//UB3LYP/6-31G(d) method, and the resulting relaxation energies are given in Table 4. It appears that the E_{rex}(angle) is always significantly larger than E_{rex}(bond). This is a consequence of a large change in hybridization from roughly sp^3 to sp^2, since all radicals are planar in their equilibrium geometries. The optimization of the bond distances in the planar structure providing E_{rex}(bond) in $\dot{C}H_3$ gives a very small stabilization of only 0.2 kcal mol^{-1}, since the bond distance is shortened by only 0.01 Å and the resonance effect is missing. The E_{rex}(bond) term assumes values of 2.4 and 5.0 kcal mol^{-1} in $\dot{C}H_2CN$ and $\dot{C}H(CN)_2$, respectively, which can be attributed to the resonance effect between the central radical center and the C≡N group. This conclusion is corroborated by the facts that the change in hybridization triggered by bond relaxation is very small (Table 4) and that the π-bond orders of the $\dot{C}$—C bonds are significantly increased compared to the bond unrelaxed values (Table 4). They are 0.43 and 0.38 in **6**$^{\bullet}$ and **7**$^{\bullet}$, respectively, as obtained by Löwdin electron density partition recipe[56] and the ROMP2/6-31G(d)//UB3LYP/6-31G(d) calculations. Concomitantly, the π-bond order in the C≡N is slightly decreased from 1.0 to 0.97 due to resonance. As a logical consequence the (C—C) bond distances are substantially shortened to 1.382 and 1.398 Å in **6**$^{\bullet}$ and **7**$^{\bullet}$, respectively, and the C≡N bonds are moderately stretched. It should be noted in passing that the C≡N groups are bent away from the $\dot{C}$—C axis by 1.0° in $\dot{C}H_2(CN)_2$ due to nitrogens repulsion. A similar stabilization between the π-orbitals of the C≡N groups and the four-membered ring takes place in the saddle points, which are diradicals. As an illustration we give four active MR-AQCC orbitals of **4** in the transition state (Figure 3) together with their natural occupation numbers as obtained by the MR-AQCC(4,4)/CASSCF(12,12)/6-31G(d) method. Two degenerate orbitals $2b_{1g}$ and $2b_{2g}$ in **4SP** are populated by 0.996 (in |e|) revealing almost perfect diradical state. They are combined with the π orbitals of the cyano carbon atoms reflecting their effective interaction. It should be noted that the fourth orbital $2a_u$ has small but significant population (0.131), which contributes to the increased π-bonding between the ring and cyano groups (Figure 3). Specifically, it increases the π-bond order between the carbon atoms of the ring and cyano group and decreases it within the triple bond, which is a signature of the resonance effect. These fine details are parts of the overall picture, which leads to small, but noticeable decrease in the barrier upon cyanation. To summarize, one can conclude that the transition (saddle) structures are stabilized relative to the equilibrium geometries in cyano derivatives of CBD due to the high diradical character of the former, which leads to enhanced resonance effect with substituents. Hence, the barriers are lower.

The calculated barrier heights for the automerization reactions and 2,3- and 1,2-dicyanocyclobutadiene bond stretch isomerism with and without the ZPVEs are summarized in Table 5. We shall discuss the former barriers. The computed MR-AQCC+ZPVE barrier for the CBD automerization is 6.4 kcal mol^{-1},

TABLE 4: Selected Structural and Bonding Parameters in the Partially Frozen Radicals and Their Completely Relaxed Forms 5•−7• as Obtained by the ROMP2/6-311+G(d,p)//UB3LYP/6-31G(d) Method[a,b]

	d(C−C)	s% (CC)	π_{bo}	d(CN)	s%(CN)	π_{bo}	d(C−H)	s%(CH)
5• (fb)							1.093	25.0
5•							1.083	33.3
6• (fb)	1.462	32.3−51.7	0.31	1.160	48.1−47.0	1.0	1.095	33.9
6•	1.382	34.5−52.6	0.43	1.177	47.2−44.9	0.97	1.084	32.8
7•(fb)	1.470	32.9−50.7	0.31	1.159	49.0−46.5	1.0	1.098	34.2
7•	1.398	34.0−51.6	0.38	1.172	48.1−44.9	0.97	1.087	32.0

[a] The bond lengths are given in Å, s characters in percent, and π-bond orders (π_{bo}) in lel. The angularly relaxed planar radicals with frozen bonds are denoted as $N^{\bullet}$ (fb), where $N = 5$, 6, and 7. [b] The relaxation energies in kcal mol^{-1} E_{rex}(angle) [E_{rex}(bond)] released by bond angle and bond distance optimization (see text), the latter being given within square parentheses. They are for **5•**, **6•**, and **7•** radicals 6.6 [0.2], 8.2 [2.4], and 9.6 [5.0] kcal mol^{-1}, respectively.

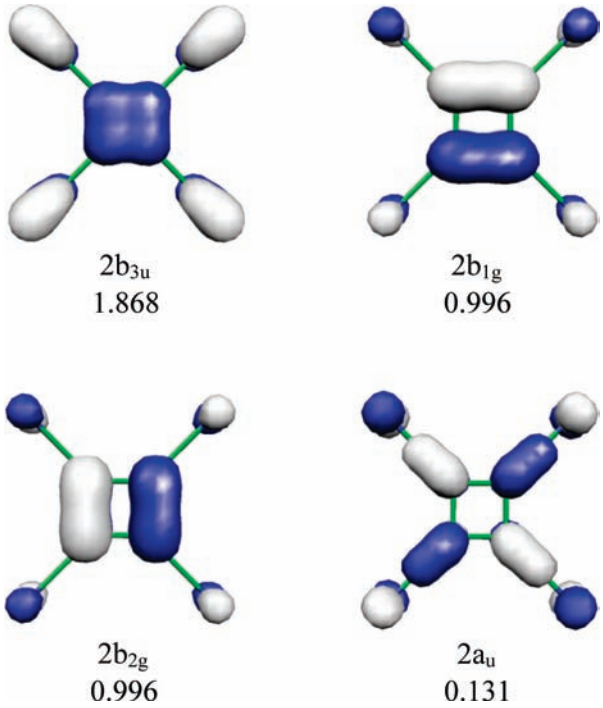

Figure 3. Four active MR-AQCC orbitals with the symmetry labels and their natural occupation numbers in the transition state for the automerization reaction of tetracyanocyclobutadiene.

TABLE 5: Calculated Barrier Heights for Automerization Reaction of Molecules 1−4 Estimated without and with ZPVE Contribution (All Values in kcal mol^{-1})[a]

barrier	CASSCF	CASSCF+ ZPVE	MR-AQCC[a]	MR-AQCC+ ZPVE	ΔE(BH)[b]
1	6.2	3.7	8.9	6.4	0.0
2	5.4	3.1	8.7	6.4	0.0
3a	4.8	2.3	7.6	5.1	1.3
3b	4.4	2.3	6.4	4.3	2.1
3c	4.2	2.1	5.7	3.6	2.8
4	3.3	1.2	4.7[c]	2.6	3.8

[a] MR-AQCC(4,4)/6-311G(2d,p)//MR-AQCC(4,4)/6-31G(d)/CASSCF/6-31G(d). [b] A decrease in the barrier heights is denoted by ΔE(BH). [c] MR-AQCC(4,4)/6-31G(2d,p)//MR-AQCC(4,4)/6-31G(d)/CASSCF/6-31G(d).

which is in excellent agreement with the recent value of 6.3 kcal mol^{-1} based on more extended MR-AQCC calculations.[21] It appears that the barrier-heights for **1**, **2**, **3a**, **3b**, **3c**, and **4** are 6.4, 6.4, 5.1, 4.3, 3.6, and 2.6 kcal mol^{-1}, respectively, meaning that the cyano groups decrease the barrier heights as conjectured above. Specifically, a decrease along the series **3a**, **3b**, **3c** and **4** is 1.3, 2.1, 2.8, and 3.8 kcal mol^{-1}, respectively. In view of the low barrier height, it is concluded that the cyano derivatives

TABLE 6: Total Electronic Energies (au) and the Difference $\Delta E(1TS)_e$ (in kcal mol^{-1}) between SPs and the LTSs of Molecules 1−3 and the Influence of the ZPVE on the Adiabatic Excitations $\Delta E(1TS)_e$ + Δ(ZPVE) (Included within Parentheses) in kcal mol^{-1}[a]

	LTS			$\Delta E(1TS)_e$[b]	
	CASSCF	MR-AQCC[a]	ZPVE	CASSCF	MR-AQCC
1	−153.68187	−154.27067	39.2	10.2 (12.4)	6.0 (8.2)
	{−153.68167}	{−154.27064}		[10.3]	[6.0]
2	−245.44985	−246.32339	38.9	10.1 (12.2)	4.4 (6.5)
	{−245.44972}	{−246.32312}		[10.2]	[4.9]
3a	−337.21097	−338.35981	37.8	10.3 (12.1)	5.6 (7.4)
	{−337.21091}	{−338.35901}		[10.3]	[6.1]
3b	−337.21116	−338.36060	38.4	9.6 (11.6)	5.1 (7.1)
	{−337.21097}	{−338.36000}		[9.7]	[5.5]
3c	−337.21013	−338.36060	38.3	10.2 (12.1)	5.1 (7.0)
	{−337.21097}	{−338.35811}		[9.7]	[6.7]

[a] MR-AQCC(4,4)/6-311G(2d,p)//MR-AQCC(4,4)/6-31G(d)/CASSCF/6-31G(d). [b] The vertical excitation ΔE(1**TS**)$_e$ energies are given within square parentheses. The total electronic energies of the E(LTS)$_e$ are calculated by using the structural parameters of the saddle point and placed within curly parentheses.

of **CBD** do not exhibit bond-stretch isomerism. Instead, they represent fluxional systems which in turn perpetually vibrate either between the two equivalent structures or between 2,3-(**3b**) and 1,2-dicyanocyclobutadiene (**3c**) isomers at room temperature.

Finally, a point of considerable interest is the energy difference between the saddle-point structure and the minimum-energy structure of the lowest triplet state. The electronic CASSCF and MR-AQCC energies for the triplet structures of compounds **1**−**3** and the corresponding ZPVEs are presented in Table 6. Unfortunately, the tetracyano derivative **4** posed a technical problem for the MR-AQCC geometry calculations of the lowest triplet state due to the computational intricacies. The adiabatic MR-AQCC excitations including the ZPVE contributions for **1**, **2**, **3a**, **3b**, and **3c** are 8.2, 6.5, 7.4, 7.1, and 7.0 kcal mol^{-1}, respectively. It appears that the gap between saddle point energy and the first triplet minimum energy structure monotonically decreases upon CN substitutions too, with the exception for the compound **2**, which has a lower S-T gap than expected. It is noteworthy that the vertical excitation energies are close to the adiabatic ones (Table 6).

Conclusions

Extended quantum chemical calculations have been performed for mono- to tetracyano-substituted cyclobutadienes with the goal of evaluating structural and energetic effects of a strong electron accepting substituent par excellence. Major interest was focused on the question how the cyano substitution affects the

energy barriers separating different bond-stretch isomers in spe. The MR-AQCC calculations used in this work show that the automerization barrier height in polycyano derivatives of CBD decreases as the number of the CN groups increases. The range of the ZPVE-corrected energy barriers lies between 2.6 (**4**), 5.1 (**3a**), and 6.4 (**1**) kcal mol^{-1} implying that cyanocyclobutadienes are fluxional molecules. Analysis of the structural data strongly indicates that diminished barrier heights by small, but significant amounts are due to the resonance effect between the ring and cyano group(s), which is more pronounced in the saddle point structures compared to that occurring in the equilibrium geometries. This is a consequence of the additional stabilization of the CN group by the diradical transition states. The results also reveal that the adiabatic energy gap between the singlet saddle point and the first triplet minimum energy structure decreases upon cyano substitutions too. The splitting is small being within the range of 6.5 − 8.2 kcal mol^{-1}.

It is hoped that the present work will induce synthesis of cyano-CBDs, since the required synthetic methods are developed and known for a long time.[57,58] This would be useful, because tetracyano-CBD would easily accommodate additional electron thus forming a stable anion[58] and possibly dianion.[59] Hence, it could provide a suitable building block in forming larger polymeric structures. Finally, one can safely conclude that the cyclobutadiene bond-stretch isomers could be expected, if the repulsion between the substituents were more pronounced in the saddle points (transition states) than in the ground state equilibrium structures. An obvious choice would be polyfluoro-CBD. Investigation of the barrier heights of the multiply substituted fluoro-cyclobutadienes is under way. Preliminary results show that fluoro-CBDs do exhibit bond stretch isomerism. This line of research is potentially useful, because the bond-stretch isomers could be helpful in designing "molecular muscles" or "molecular switches.[60,61] In contrast, use of acetylene fragments as substituents would diminish the barrier height just like in the case of the cyano group.

Acknowledgment. The authors acknowledge financial support by the WTZ treaty between Austria and Croatia (Project No. 1/2006). The work in Austria (H.L.) was also supported by the Austrian Science Fund within the framework of the Special Research Program F16 (ADLIS) and Project No. P18411-N19, while the work in Zagreb (M.E.-M., M.V., and Z.B.M.) was supported by the Ministry of Science and Technology of Croatia (Project Nos. 098-0982933-2920 and 098-0982933-2932). This work was also sponsored by the COST D37 action, working group 0001-06PhotoDyn. Support (H.L.) by the grant from the Ministry of Education of the Czech Republic (Center for Biomolecules and Complex Molecular Systems, LC512) and by the Praemium Academiae of the Academy of Sciences of the Czech Republic, awarded to Pavel Hobza in 2007, is gratefully acknowledged. The work of H.L. was part of the research project Z40550506 of the Institute of Organic Chemistry and Biochemistry of the Academy of Sciences of the Czech Republic. The calculations were performed in part on the Schrödinger III Linux cluster of the Vienna University Computer Center. We would like to thank the editors for their stimulating and very useful comments.

Supporting Information Available: Tables of the s character of the local NBO hybrid orbitals calculated by different theoretical methods, s characters obtained by NBO method as calculated by the B3LYP/6-311G(d) scheme, and imaginary frequencies for the isomerization reactions of molecules **1**−**4** as obtained by the CASSCF/6-31G(d) method and an illustration of the resonance effect in **3a** and **3c** including the most important zwitterionic structures. This material is available free of charge via the Internet at http://pubs.acs.org.

References and Notes

(1) Baeyer, A. *Ber. Dtsch. Chem. Ges.* **1885**, *18*, 2269.
(2) Breslow, R.; Brown, J.; Gajewski, J. J. *J. Am. Chem. Soc.* **1967**, *89*, 4383.
(3) Breslow, R. *Acc. Chem. Res.* **1973**, *6*, 393.
(4) Eckert-Maksić, M.; Maksić, Z. B. In *The Chemistry of Cyclobutanes*; Rappoport, Z., Liebman, J. F., Eds.; John Wiley: Chichester, 2005; p 16.
(5) Fattahi, A.; Lis, L.; Tian, Z.; Kass, S. R. *Angew. Chem., Int. Ed. Engl.* **2006**, *45*, 4984.
(6) Bally, T.; Masamune, S. *Tetrahedron* **1980**, *36*, 343.
(7) Stohrer, W. D.; Hoffmann, R. *J. Am. Chem. Soc.* **1972**, *94*, 1661.
(8) Gibson, V. C.; McPartlin, M. *J. Chem. Soc., Dalton Trans.* **1992**, 947.
(9) Parkin, G. *Chem. Rev.* **1993**, *93*, 887.
(10) Rohmer, M.-M.; Benard, M. *Chem. Soc. Rev.* **2001**, *30*, 340.
(11) Goldman, G. D.; Roberts, B. E.; Cohen, T. D.; Lemal, D. M. *J. Org. Chem.* **1994**, *59*, 7421.
(12) Niecke, E.; Fuchs, A.; Nieger, M. *Angew. Chem., Int. Ed. Engl.* **1999**, *38*, 3028.
(13) Schoeller, W. W.; Begemann, C.; Niecke, E.; Gudat, D. *J. Phys. Chem. A* **2001**, *105*, 10731.
(14) Sebastian, M.; Nieger, M.; Szieberth, D.; Nyulaszi, L.; Niecke, E. *Angew. Chem., Int. Ed. Engl.* **2004**, *43*, 637.
(15) Rodriguez, A.; Olsen, R. A.; Ghaderi, N.; Scheschkewitz, D.; Tham, T. S.; Mueller, L. J.; Bertrand, G. *Angew. Chem., Int. Ed. Engl.* **2004**, *43*, 4880.
(16) Antol, I.; Eckert-Maksić, M.; Lischka, H.; Maksić, Z. B. *ChemPhysChem* **2004**, *5*, 975.
(17) Borden, W. T.; Davidson, E. R. *J. Am. Chem. Soc.* **1980**, *102*, 7958.
(18) Arnold, B. R.; Michl, J. *J. Phys. Chem.* **1993**, *97*, 13348.
(19) Whitman, D. W.; Carpenter, B. K. *J. Am. Chem. Soc.* **1982**, *104*, 6473.
(20) Carpenter, B. K. *J. Am. Chem. Soc.* **1983**, *105*, 1700.
(21) Eckert-Maksić, M.; Vazdar, M.; Barbatti, M.; Lischka, H.; Maksić, Z. B. *J. Chem. Phys.* **2006**, *125*, 064310.
(22) Demel, O.; Pittner, J. *J. Chem. Phys.* **2006**, *124*, 144112.
(23) Balková, A.; Bartlett, R. J. *J. Chem. Phys.* **1994**, *101*, 8972.
(24) Maier, G.; Kalinowski, H. O.; Euler, K. *Angew. Chem., Int. Ed. Engl.* **1982**, *21*, 693.
(25) Mediavilla, C.; Tortajada, J.; Baonza, V. G. *Chem. Phys. Lett.* **2008**, *454*, 387.
(26) Ruedenberg, K.; Cheung, L. M.; Elbert, S. T. *Int. J. Quantum Chem.* **1979**, *16*, 1069.
(27) Roos, B. O. *Adv. Chem. Phys.* **1987**, *69*, 399.
(28) Roos, B. O.; Taylor, P. R.; Sigbahn, P. E. M. *Chem. Phys.* **1980**, *48*, 157.
(29) Lischka, H.; Dallos, M.; Shepard, R. *Mol. Phys.* **2002**, *100*, 1647.
(30) Shepard, R. The Analytic Gradient Method for Configuration Interaction Wave Functions. In *Modern Electronic Structure Theory*; Yarkony, D. R., Ed.; World Scientific: Singapore, 1995; Vol. 1, p 345.
(31) Shepard, R.; Lischka, H.; Szalay, P. G.; Kovar, T.; Ernzerhof, M. *J. Chem. Phys.* **1992**, *96*, 2085.
(32) Bunge, A. *J. Chem. Phys.* **1970**, *53*, 20.
(33) Fogarasi, G.; Zhou, X. F.; Taylor, P. W.; Pulay, P. *J. Am. Chem. Soc.* **1992**, *114*, 8191.
(34) Csaszar, P.; Pulay, P. *J. Mol. Struct.* **1984**, *114*, 31.
(35) Hehre, W. J.; Ditchfield, R.; Pople, J. A. *J. Chem. Phys.* **1972**, *56*, 2257.
(36) Pulay, P.; Fogarasi, G.; Pongor, G.; Boggs, J. E.; Vargha, A. *J. Am. Chem. Soc.* **1983**, *105*, 7037.
(37) Lischka, H.; Shepard, R.; Brown, F. B.; Shavitt, I. *Int. J. Quantum Chem.* **1981**, *S15*, 91.
(38) Shepard, R.; Shavitt, I.; Pitzer, R. M.; Comeau, D. C.; Pepper, M.; Lischka, H.; Szalay, P. G.; Ahlrichs, R.; Brown, F. B.; Zhao, J. G. *Int. J. Quantum Chem., Quantum Chem. Symp.* **1988**, *22*, 149.
(39) Lischka, H.; Shepard, R.; Shavitt, I.; Pitzer, R. M.; Dallos, M.; Müller, T.; Szalay, P. G.; Brown, F. B.; Ahlrichs, R.; Boehm, H. J.; Chang, A.; Comeau, D. C.; Gdanitz, R.; Dachsel, H.; Ehrhardt, C.; Ernzerhof, M.; Höchtl, P.; Irle, S.; Kedziora, G.; Kovar, T.; Parasuk, V.; Pepper, M. J. M.; Scharf, P.; Schiffer, H.; Schindler, M.; Schüler, M.; Seth, M.; Stahlberg, E. A.; Zhao, J.-G.; Yabushita, S.; Zhang, Z.; Barbatti, M.; Matsika, S.; Schuurmann, M.; Yarkony, D. R.; Brozell, S. R.; Beck, E. V.; Blaudeau, J.-P. *COLUMBUS, an ab initio electronic structure program*, release 5.9.1 2006; www.univie.ac.at/columbus.

(40) Lischka, H.; Shepard, R.; Pitzer, R. M.; Shavitt, I.; Dallos, M.; Müller, T.; Szalay, P. G.; Seth, M.; Kedziora, G. S.; Yabushita, S.; Zhang, Z. Y. *Phys. Chem. Chem. Phys.* **2001**, *3*, 664.

(41) Helgaker, T.; Jensen, H. J. A.; Jørgensen, P.; Olsen, J.; Ruud, K.; Ågren, H.; Andersen, T.; Bak, K. L.; Bakken V.; Christiansen, O.; Dahle, P.; Dalskov, E. K.; Enevoldsen, T.; Heiberg, H.; Hettema, H.; Jonsson, D.; Kirpekar, S.; Kobayashi, R.; Koch, H.; Mikkelsen, K. V.; Norman, P.; Packer, M. J.; Saue, T.; Taylor, P. R.; Vahtras, O. *DALTON, an ab initio electronic structure program*; release 1.0 1997.

(42) Frisch, M. J.; Trucks, G. W.; Schlegel, H. B.; Scuseria, G. E.; Robb, M. A.; Cheeseman, J. R.; Montgomery, J. J. A.; Vreven, T.; Kudin, K. N.; Burant, J. C.; Millam, J. M.; Iyengar, S. S.; Tomasi, J.; Barone, V.; Mennucci, B.; Cossi, M.; Scalmani, G.; Rega, N.; Petersson, G. A.; Nakatsuji, H.; Hada, M.; Ehara, M.; Toyota, K.; Fukuda, R.; Hasegawa, J.; Ishida, M.; Nakajima, T.; Honda, Y.; Kitao, O.; Nakai, H.; Klene, M.; Li, X.; Knox, J. E.; Hratchian, H. P.; Cross, J. B.; Bakken, V.; Adamo, C.; Jaramillo, J.; Gomperts, R.; Stratmann, R. E.; Yazyev, O.; Austin, A. J.; Cammi, R.; Pomelli, C.; Ochterski, J. W.; Ayala, P. Y.; Morokuma, K.; Voth, G. A.; Salvador, P.; Dannenberg, J. J.; Zakrzewski, V. G.; Dapprich, S.; Daniels, A. D.; Strain, M. C.; Farkas, O.; Malick, D. K.; Rabuck, A. D.; Raghavachari, K.; Foresman, J. B.; Ortiz, J. V.; Cui, Q.; Baboul, A. G.; Clifford, S.; Cioslowski, J.; Stefanov, B. B.; Liu, G.; Liashenko, A.; Piskorz, P.; Komaromi, I.; Martin, R. L.; Fox, D. J.; Keith, T.; Al-Laham, M. A.; Peng, C. Y.; Nanayakkara, A.; Challacombe, M.; Gill, P. M. W.; Johnson, B.; Chen, W.; Wong, M. W.; Gonzalez, C.; Pople, J. A. *Gaussian 03*, revision C.02; Gaussian, Inc., Wallingford CT 2004.

(43) Foster, J. P.; Weinhold, F. *J. Am. Chem. Soc.* **1980**, *102*, 7211.

(44) Reed, A. E.; Weinhold, F. *J. Chem. Phys.* **1983**, *78*, 4066.

(45) Maksić, Z. B. In *Theoretical Models of Chemical Bonding*; Maksić, Z. B., Ed.; Springer Verlag: Berlin-Heidelberg, 1990; Vol. 2; p 137.

(46) Bent, H. A. *Chem. Rev.* **1961**, *61*, 275.

(47) Maksić, Z. B.; Eckert-Maksić, M.; Rupnik, K. *Croat. Chem. Acta* **1984**, *57*, 1295.

(48) Kovačević, K.; Maksić, Z. B. *J. Org. Chem.* **1974**, *39*, 539.

(49) Maksić, Z. B.; Rubčić, A. *J. Am. Chem. Soc.* **1977**, *99*, 4233.

(50) Flanigan, M. C.; Kormornicki, A.; McIver, J. W. J. In *Electronic Structure Calculations*; Segel, A. G., Ed.; Plenum Press: New York, 1977.

(51) Schulman, J. M.; Disch, R. L. *Chem. Phys. Lett.* **1985**, *113*, 291.

(52) Ibrahim, M. R.; Fataftah, Z. A. *Chem. Phys. Lett.* **1986**, *125*, 149.

(53) Barić, D.; Maksić, Z. B.; Vianello, R. *THEOCHEM* **2004**, *672*, 201.

(54) King, W. T. *J. Chem. Phys.* **1972**, *57*, 4535.

(55) Rysnik-Gaughan, R.; King, W. T. *J. Chem. Phys.* **1972**, *57*, 4530.

(56) Löwdin, P. O. *J. Chem. Phys.* **1950**, *18*, 63.

(57) Webster, O. W. *J. Polym. Sci: Part A: Polym. Chem.* **2002**, *40*, 210.

(58) see Vianello, R.; Maksić, Z. B. *New J. Chem.* **2009**, *33*, 739.

(59) Despotović, I.; Maksić, Z. B. *THEOCHEM* **2007**, *811*, 313.

(60) Marsella, M. J. *Acc. Chem. Res.* **2002**, *35*, 944.

(61) Berson, J. A. *Acc. Chem. Res.* **1997**, *30*, 238.

JP9015273